EZH2/EHMT2 Histone Methyltransferases Inhibit the Transcription of DLX5 and Promote the Transformation of Myelodysplastic Syndrome to Acute Myeloid Leukemia

Zhuanzhe Zheng
Shanxi Medical University Second Affiliated Hospital: Second Hospital of Shanxi Medical University
Ling Li
Shanxi Medical University Second Affiliated Hospital: Second Hospital of Shanxi Medical University
Guoxia Li
Shanxi Medical University Second Affiliated Hospital: Second Hospital of Shanxi Medical University
Yaofang Zhang
Shanxi Medical University Second Affiliated Hospital: Second Hospital of Shanxi Medical University
Chunxia Dong
Shanxi Medical University Second Affiliated Hospital: Second Hospital of Shanxi Medical University
Fanggang Ren
Shanxi Medical University Second Affiliated Hospital: Second Hospital of Shanxi Medical University
Wenliang Chen
Shanxi Medical University Second Affiliated Hospital: Second Hospital of Shanxi Medical University
Yanping Ma (yanpm1106@163.com)
Shanxi Medical University Second Affiliated Hospital: Second Hospital of Shanxi Medical University
https://orcid.org/0000-0002-9416-1870

Research

Keywords: Myelodysplastic syndromes, Acute myeloid leukemia, EZH2, EHMT2, DLX5, H3K27me3, H3K9me2

Posted Date: December 3rd, 2020

DOI: https://doi.org/10.21203/rs.3.rs-117131/v1

Abstract

Objective

Myelodysplastic syndrome (MDS) is a group of heterogeneous myeloid clonal diseases originating from hematopoietic stem cells and may develop to acute myeloid leukemia (AML). We investigated the mechanism of histone methyltransferases EZH2/EHMT2 during the transformation of MDS to AML.

Methods

Expression of EZH2/EHMT2 in MDS/AML patients and in NHD13 mice was detected. EZH2 and EHMT2 were silenced or overexpressed in SKM-1 cells to evaluate cell proliferation and cycle. Levels of DLX5, H3K27me3 and H3K9me2 were detected. The binding of DLX5 promoter region to H3K27me3 and H3K9me2 was examined. Levels of H3K27me3/H3K9me2 in cells were decreased by EZH2/EHMT2 inhibitors, and then changes of DLX5 expression and cell proliferation were observed.

Results

EZH2 was poorly expressed in MDS patients but highly expressed in MDS-AML patients. EHMT2 was elevated in both MDS and MDS-AML patients. EZH2 expression was reduced and EHMT2 expression was promoted in NHD13 mice. NHD13 mice with overexpressing EZH2 or EHMT2 transformed into AML more quickly. Intervention of EZH2 or EHMT2 inhibited SKM-1 cell proliferation and promoted DLX5 expression. Both silencing EZH1 and EZH2 in SKM-1 cells, the H3K27me3 level was decreased. EZH2 silencing repressed the proliferation of SKM-1 cells. The transcription level of DLX5 in SKM-1 cells was inhibited by H3K27me3 and H3K9me2. Enhanced DLX5 expression restrained the proliferation of SKM-1 cells.

Conclusion

EZH2/EHMT2 catalyzed H3K27me3/H3K9me2 to inhibit the transcription of DLX5, thus promoting the transformation from MDS to AML.

Introduction

Myelodysplastic syndrome (MDS) comprises a group of heterogeneous myeloid neoplasms sharing the common characteristics of bone marrow failure, including hematopoietic dysfunction, morphologic dysplasia and peripheral blood cell reduction [1]. MDS patients with multiple lineage cytopenias, high percentage of bone marrow blasts or characteristic chromosomal abnormalities, usually develop rapidly into acute myeloid leukemia (AML) and eventually die of the disease in the absence of bone marrow transplantation [2]. AML is a completely malignant and aggressive blood cancer, featured by the extensive accumulation of developmentally arrested and immature blasts in bone marrow [3]. It has demonstrated that more than half of MDS and AML cases are the elderly, and the prevalence of MDS and AML may continue increasing due to the global population aging [4]. Identifying the potential molecular

events associated with MDS/AML progression can better understand the pathogenesis of this disease and improve the therapeutic effect.

Epigenetics refers to the presence of heritable phenotypes that produce heritable information in genetic functions without changing DNA sequence, which participates in the growth, disease and death of organisms together with traditional genetic information [5]. As a form of epigenetic modification, histone methylation plays a vital part in gene transcription regulation and disease progression by affecting the densification of chromatin histone tails and binding of proteins such as the transcription factors that identify histone markers [6]. Emerging evidence has revealed that abnormal histone methylation is concerned with the occurrence and progression of MDS [7]. Histone H3 and H4 represent the most common methylation sites and the methylation of each site is catalyzed by a special enzyme named methyltransferase [5]. Intriguingly, the application of methyltransferase inhibitors for MDS patients has altered the landscape of this disease and produced benign clinical benefits [8].

EZH2 is a histone methyltransferase, which can tri-methylate histone H3 of lysine 27 (H3K27me3) and silence target genes related to various functions including cell cycle, proliferation and differentiation [9]. The aberrant expression of EZH2 is closely related to the transformation from MDS to AML, which consequently may become a potential biomarker of MDS evolution [10]. Goro Sashida et al. have shown that EZH2 deletion accelerates the development of MDS, but weakens the tendency of MDS to AML [11]. EHMT2 is partly responsible for the mono- and di-methylation of histone H3 lysine 9 (H3K9me1 and H3K9me2, respectively) [12]. EHMT2 is promoted and amplified in a variety of cancers including leukemia, prostate cancer and lung cancer, and knockdown of EHMT2 can repress the growth of these cancer cells [13–15]. Importantly, a recent literature has exhibited that EHMT2 and EZH2 interact physically and share targets for epigenetic silencing [16]. The dual inhibition of EZH2 and EHMT2 can induce gene transcription and inhibit tumor cell growth more effectively [17]. However, the epigenetic regulation mechanism of EZH2/EHMT2 in the transformation of MDS remains unclear yet. We herein explored the effect of EZH2/EHMT2 on the transformation from MDS to AML, which shall provide a theoretical basis for the management of MDS and MDS-AML.

Materials And Methods

Ethics statement

The study got the approval of the Clinical Ethical Committee of The Second Hospital of Shanxi Medical University. Informed consent was signed by each eligible participant.

Tissue samples

Thirty-three bone marrow samples were collected from The Second Hospital of Shanxi Medical University from 2015 to 2018. All the samples were confirmed as MDS (n = 11), MDS-AML (n = 11) or cancer-free individuals (n = 11) by bone marrow puncture and/or biopsy. Bone marrow samples were extracted with human peripheral blood lymphocyte separation solution (TBD, Tianjin, China) by density gradient

method. Total RNA was isolated from monocytes using RNAiso Plus reagent (Takara, Dalian, China) and reverse transcribed into cDNA using a reverse transcription quantitative polymerase chain reaction kit (Takara), and then stored at -80℃.

Experimental animals

NHD13 mice were purchased from Jackson Laboratory and C57BL/6 mice were purchased form Kunming Institute of Zoology, Chinese Academy of Sciences [SYXK (Yunnan) K2015-0003]. Mice were raised in a specific pathogen-free animal facility. Food and water were provided ad libitum. The expressions of EZH2 and EHMT2 in peripheral blood of mice were detected at 4 months old. Then peripheral blood was collected regularly and the blood condition was detected. Blood samples were collected from mice at the age of 14 months (420 days), and then all the mice were euthanized by an intraperitoneal injection of pentobarbital (800 mg/kg) [18, 19].

Cell culture

Human MDS/AML cells (SKM-1 cells) were purchased from American Type Culture Collection (Manassas, VG, USA) and cultured in Roswell Park Memorial Institute-1640 medium containing 10% fetal bovine serum in a 95% humidified air with 5% CO_2 at 37℃.

The small interfering RNA (siRNA)-NC-1, si-EZH1, si-NC-2, si-EZH2, si-NC-T2 and si-EHMT2 were designed and synthesized. Overexpression vectors of EZH2 (pcDNA3.1-EZH2) and EHMT2 (pcDNA3.1-EHMT2) were constructed, with the empty vectors as loading control. Then, the constructed vectors and siRNAs were transfected into cells using Lipofectamine 2000 (Invitrogen Inc., Carlsbad, CA, USA). And SKM-1 cells were treated with PF-06726304 (15 nM; MedChemExpress, NJ, USA) or BRD4770 (5 nM; MedChemExpress) respectively, with the treated cell named as PF group and BRD group, respectively.

Cell counting kit-8 (CCK-8) assay

The treated cells were seeded into the 96-well plates (2×10^3 cells/well), and CCK-8 solution was added at 24, 48 and 72 h. The optical density of each well was measured at 450 nm. The experiment was repeated three times in each group.

Flow cytometry

SKM-1 cells or KG-1 cells under different treatments were fixed with 70% ethanol, stained with 300 mL propidium iodide (MultiSciences Biotech Co., Ltd, Hangzhou, Zhejiang, China) in the dark and detected on the flow cytometer (MoFloAstrios EQ, Beckman Coulter, Inc., CA, USA) to analyze the cell cycle.

5-ethynyl-2’-deoxyuridine (EdU) labeling assay

SKM-1 cells or KG-1 cells under different treatments were removed from the culture medium, washed with phosphate-buffered saline (PBS), incubated with EdU solution for 2 h, and then photographed under a fluorescence microscope (Olympus, Tokyo, Japan).

Colony formation assay

SKM-1 cells or KG-1 cells under different treatments were seeded into the 12-well plates (1×10^4 cells/well), and incubated at 37℃ for one week until cell colonies were observed. The colonies were stained with crystal violet and counted.

Chromatin immunoprecipitation (ChIP)

SKM-1 cells were subjected to ChIP assay referring to a previous literature [20]. Cells were detached with trypsin and counted using Millipore Scepter 2.0 Cell (Thermo Fisher Scientific, Jiangsu, China). And 1×10^6 cells were used for each treatment. Cells were incubated for 8 min in the medium, fixed with formaldehyde and then crosslinked with 1.25 M glycine for 5 min at room temperature. All chromatin preparation and ChIP reaction were carried out at 4℃. The crosslinked cells were washed with PBS-inhibitor (NaBu 20 mM), and the cell membrane was cleaved with the HighCell ChIP kit. Chromatin was prepared in TPX tube with shear buffer S1 and 1 × protease inhibitor, and then treated into fragments of about 500 bp by ultrasound. The size of the fragments was examined on agarose gel, and the cut chromatin was frozen at -80℃. ChIP reaction was performed using the Diagenode kit on the SX-8X IP STAR compact automation system (Diagenode) for all IP procedures. According to the HighCell ChIP kit protocol, IP DNA was purified using DNA Isolation buffer with 2 μg antibody (anti-H3K27me3 or anti-H3K9me1 or anti-H3K9me2) and non-immune immunoglobulin G (IgG). Each auto-ChIP sample was performed using the Auto Histone ChIP-seq kit and contained 1 μg input chromatin. The reaction lasted for 2 h. The antibody was coated with protein A-coated magnetic beads, and then incubated for 10 h at 4 °C for IP reaction. Afterwards, 25 μL system of DNA IP or DNA input (total DNA), 1 × SYBR Green Supermax (Applied Biosystems, Inc., Carlsbad, CA, USA) and TSH2B (pp-1041–500, Diagenode; positive control of methylation) promoter were used for reverse transcription quantitative polymerase chain reaction (RT-qPCR), with the sequence of DLX5 promoter region as primer.

RT-qPCR

Total RNA was extracted from cells using TRIzol one-step reagent (Invitrogen), and then the concentration and purity of RNA were determined using UV analysis and formaldehyde deformation electrophoresis. The fluorescent qPCR reaction was performed on the instructions of the RT-qPCR kit (ThermoFisher scientific). Primers (Table 1) were designed and synthesized by Sangon Biotech (Shanghai, China). Amplification curve and dissolution curve were confirmed after reaction. The relative expression of genes was calculated by $2^{-\Delta\Delta Ct}$ method, with glyceraldehyde-3-phosphate dehydrogenase (GAPDH) as the internal reference.

Table 1
Primer sequence for RT-qPCR

Gene	Primer sequence
GAPDH	F: 5'-GGGAGCCAAAAGGGTCAT-3'
	R: 5'-GAGTCCTTCCACGATACCAA-3'
EZH2	F: 5'-ATGGGCCAGACTGGGAAGAAA-3'
	R: 5'-GGAGGTAGCAGATGTCAAGGG-3'
EZH1	F: 5'-ATGGAGGATTACAGCAAGATGG-3'
	R: 5'-GGGGCCTGGGAGGGCTAAAGGA-3'
EHMT2	F: 5'-ATGCGGGGTCTACCGAGAGGG-3'
	R: 5'-AGAGAGGGTGTGGTCCGTTCTC-3'
DLX5	F: 5'-ATGACAGGAGTGTTTGACAGAAG-3'
	R: 5'-CTAATAGAGTGTCCCGGAGGCCA-3'
Hoxa9	F: 5'-ATGGCCACCACTGGGGCCCTGGGC-3'
	R: 5'-GCCCAAATGGCATCACTCGTCTTT-3'

Western blot analysis

Cells in each group were lysed in radio-immunoprecipitation assay buffer containing protease inhibitors (Sigma-Aldrich, Merck KGaA, Darmstadt, Germany). The lysate was centrifuged at 16000 g and 4 °C for 20 min to collect the supernatants. The concentration of protein extracted from cells was tested using the Pierce bicinchoninic acid assay kit (Beyotime, Shanghai, China). Then, the protein was separated using sodium dodecyl sulfate-polyacrylamide gel electrophoresis and transferred onto polyvinylidene difluoride membranes (Millipore, Bedford, MA, USA). The membranes were blocked with 5% skim milk for 2 h and cultured with the primary antibodies at 4 °C overnight. Thereafter, the membranes were cultured with the secondary antibody for 1 h, and developed and visualized using the enhanced chemiluminescence reagent. The gray value of the target band was analyzed by Image J software (National Institutes of Health, Maryland, USA). The antibodies used were as follows: H3K27me3 (1:1000, ab6002, Abcam, Cambridge, MA, USA), β-actin (1:1000, ab8227, Abcam), H3K9me1 (1:1000, ab9045, Abcam), H3K9me2 (1:1000, ab1220, Abcam), EZH1 (1:1000, ab189833, Abcam), EHMT2 (1:1000, ab185050, Abcam) and Hoxa9 (1:1000, ab140631, Abcam).

Statistical analysis

SPSS 21.0 (IBM Corp., Armonk, NY, USA) was utilized for data analysis. Kolmogorov-Smirnov test showed that the data were in normal distribution and expressed as mean ± standard deviation. The *t* test was adopted for analysis of comparisons between two groups. The one-way or two-way analysis of variance

(ANOVA) was applied for comparisons among multi-groups. Tukey's multiple comparison test was applied for the post hoc test after ANOVA. The p value was obtained from a two-tailed test, and $p < 0.05$ meant a statistical difference.

Results

EZH2 was downregulated in MDS patients and upregulated in MDS-AML patients

The detection of bone marrow samples collected from MDS and MDS-AML patients in The Second Hospital of Shanxi Medical University from 2015 to 2018 showed that EZH2 expression in bone marrow of MDS patients was notably lower than that of healthy non-cancer individuals ($p < 0.05$; Fig. 1A), but EZH2 expression in MDS-AML patients showed a trend of high expression ($p < 0.05$; Fig. 1B). EHMT2 was always highly expressed in MDS and MDS-AML patients (both $p < 0.05$; Fig. 1A/B). The general information of participants is shown in Table 2.

Table 2
General information of the cases

	Normal (n = 11)	MDS (n = 11)	MDS-AML (n = 11)	*p*
Age	50.5 ± 10.5	47.4 ± 12.4	51.8 ± 13.8	ns
Sex				ns
Male	6	7	7	
Female	5	4	4	
BMI (kg/m^2) Mean ± SD	22.35 ± 2.01	23.16 ± 1.97	23.51 ± 1.59	ns
Note: ns: no statistical difference				

NHD13 mice with high expression of EZH2 transformed into AML more quickly

NHD13 mice faithfully reproduced all the key features of MDS, including decreased peripheral blood cells, abnormal bone marrow hyperplasia and increased apoptosis, and conversion to acute leukemia at 4–14 months of age [21, 22]. NHD13 mice (n = 25) were observed, and the expressions of EZH2 and EHMT2 in peripheral blood of mice (at the age of four months) was detected. We showed that EZH2 expression in NHD13 mice was lower than that in healthy C57BL/6 mice ($p < 0.05$; Fig. 2A). According to the median expression of EZH2 in NHD13 mice, the mice with the expression of EZH2 higher than the median were classified as the high EZH2 group, and the mice with the expression of EZH2 lower than the median were classified as the low EZH2 group. Comparing the two groups of mice, it was found that EZH2 expression

was related to the time of NHD13 mice transforming from MDS to AML. NHD13 mice with high expression of EZH2 rapidly transformed from MDS to AML in a short period of time, while the mice with low expression of EZH2 took a relatively long time to transform into AML, even without AML transformation (Fig. 2B). Additionally, the survival rate of NHD13 mice with high EZH2 expression was significantly lower ($p < 0.05$; Fig. 2C). EHMT2 expression in NHD13 mice was notably increased compared with that in healthy mice ($p < 0.05$; Fig. 2A). Similarly, mice were grouped by the median of EHMT2 expression. It was found that mice with high expression of EHMT2 developed from MDS to AML more quickly (Fig. 2B), and the survival rate of NHD13 mice with high EHMT2 expression was significantly lower ($p < 0.05$; Fig. 2C). We also found that the EHMT2 expression of mice in the high EZH2 group was higher than that in the low EZH2 group ($p < 0.05$; Fig. 2D). These results suggested that the expressions of EZH2 and EHMT2 were related to the transformation from MDS to AML, and EZH2 and EHMT2 might have a synergistic relationship.

Interference of EZH2 expression inhibited SKM-1 cell proliferation

Our data showed that EZH2 had an opposite trend in MDS and AML. To further investigate the role of EZH2 in MDS and MDS-AML, we transfected SKM-1 cells with si-EZH2 or overexpression vector of EZH2 (pcDNA3.1-EZH2). The expression of EZH2 after transfection was verified by RT-qPCR ($p < 0.05$; Fig. 3A). SKM-1 cells transfected with si-EZH2 showed significantly reduced proliferation ability and blocked cell cycle, while SKM-1 cells transfected with pcDNA3.1-EZH2 had the opposite trend (all $p < 0.05$; Fig. 3B-E). Additionally, the expression of leukemia associated Hoxa9 in SKM-1 cells was detected. It implied that the stronger the proliferation ability of SKM-1 cells, the higher the expression of Hoxa9 ($p < 0.05$; Fig. 3F). The deletion of EZH2 inhibited MDS cell proliferation, while the overexpression of EZH2 facilitated MDS cell proliferation, and excessive proliferation promoted the accumulation of Hoxa9.

Interference of EHMT2 expression inhibited SKM-1 cell proliferation

SKM-1 cells were also transfected with si-EHMT2. The expression of EHMT2 after transfection was verified by RT-qPCR ($p < 0.05$; Fig. 4A). Compared with the untransfected cells, SKM-1 cells transfected with si-EHMT2 showed notably reduced proliferation ability and blocked cell cycle (all $p < 0.05$; Fig. 4B-E). Similarly, Hoxa9 expression was decreased with the reduction of proliferation in SKM-1 cells transfected with si-EHMT2 (Fig. 4F/G). Briefly, silencing EHMT2 expression inhibited SKM-1 cell proliferation and Hoxa9 expression.

EZH2 regulated H3K27me3 level and EZH1 compensated for the effect of EZH2 deficiency

EZH2 is an epigenetic regulator that regulates gene transcription by promoting H3K27me3 methylation level [23]. We detected H3K27me3 level in SKM-1 cells. The results revealed that H3K27me3 level was increased notably in SKM-1 cells overexpressing EZH2, but maintained a certain level in SKM-1 cells transfected with si-EZH2 ($p > 0.05$; Fig. 5A/B), which might result from the functional compensation of EZH1 [24]. Therefore, we detected EZH1 expression in cells to verify the functional compensation of EZH1 to EZH2, and identified that EZH1 expression was increased notably in the absence of EZH2 ($p < 0.05$; Fig. 5D).

Then SKM-1 cells were transfected with si-EZH1. The expression of EZH1 after transfection was verified by RT-qPCR ($p < 0.05$; Fig. 5C). We observed that downregulation of EZH2 reduced the level of HK27me3 in SKM-1 cells after reducing the compensation mechanism of EZH1 to EZH2 ($p < 0.05$; Fig. 5A/B).

EHMT2 positively regulated H3K9me1/H3K9me2 level

Similar to EZH2, EHMT2 inhibits the transcription of tumor suppressor genes by promoting the methylation and dimethylation of H3K9me1/3K9me2 [25]. We detected the levels of H3K9me1 and H3K9me2 in SKM-1 cells. H3K9me1 and H3K9me2 were decreased significantly in SKM-1 cells transfected with si-EHMT2 ($p < 0.001$) (Fig. 6).

EZH2 and EHMT2 synergistically inhibited DLX5 gene transcription

The high methylation and low expression of DLX5 are frequent in AML and MDS, and are related to the transformation from MDS to AML [26]. We detected the transcription level of DLX5 in SKM-1 cells of each group and found that transfection of si-EZH2 alone or si-EHMT2 alone could promote the DLX5 mRNA level (Fig. 7A). DLX5 mRNA level in NHD13 mice was lower than that in healthy C57BL/6 mice (Fig. 7B). DLX5 mRNA level was increased to the highest level when EZH2 and EHMT2 were at low expressions at the same time, and decreased to the lowest level when EZH2 and EHMT2 were at high expressions (Fig. 7C) (all $p < 0.001$). Therein, we speculated that the transcription of DLX5 was co-inhibited by EZH2 and EHMT2.

To confirm the specific mechanism of EZH2 and EHMT2 regulating DLX5 transcription, we detected the binding levels of DLX5 promoter region with H3K27me3, H3K9me1 and H3K9me2 in SKM-1 cells. The binding level of H3K27me3 and H3K9me2 to DLX5 promoter was significantly decreased in SKM-1 cells transfected with si-EZH2 or si-EHMT2, while the binding rate of H3K9me1 to DLX5 promoter was not affected by si-EHMT2 ($p < 0.05$) (Fig. 7D). These results indicated that EZH2 and EHMT2 synergistically catalyze H3K27me3 and H3K9me2 to inhibit DLX5 transcription in SKM-1 cells.

Then EZH1-treated SKM-1 cells were simultaneously transfected with overexpressing EZH2 and EHMT2 or silencing EZH2 and EHMT2 (Fig. 7E), which made H3K27me3 and H3K9me2 increase or decrease simultaneously (Fig. 7F). The mRNA level of DLX5 was decreased in the cells overexpressing EZH2 and

EHMT2, but increased in the cells silencing EZH2 and EHMT2 (all $p < 0.001$) (Fig. 7G). Taken together, EZH2 and EHMT2 synergistically inhibited DLX5 gene transcription in SKM-1 cells.

Histone demethylation enhanced DLX5 expression and inhibited SKM-1 cell proliferation

To verify that the transcription of DLX5 was co-inhibited by H3K27me3 and H3K9me2, we transfected the inhibitors of H3K27me3 or H3K9me2 into SKM-1 cells overexpressing EZH2 and EHMT2. DLX5 mRNA level was increased whether H3K27me3 or H3K9me2 was inhibited alone, but the increase of DLX5 mRNA level was the highest when H3K27me3 and H3K9me2 were inhibited at the same time (Fig. 8A/B). The increase of DLX5 expression inhibited the proliferation of SKM-1 cells (Fig. 8C), and the expression of Hoxa9 was negatively correlated with the expression of DLX5 (all $p < 0.001$; Fig. 8D). All in all, EZH2 and EHMT2 synergistically inhibited the transcription of DLX5 in MDS cells and promoted the transformation from MDS to AML.

Discussion

MDS has a high tendency to developing into AML and shows a poor outcome especially in the relapsed and older patients [27, 28]. Epigenetic dysregulation has been considered to be associated with the pathogenesis of MDS/AML [23]. Histone methyltransferase is an epigenetic regulator, and its potential therapeutic effect in MDS as a small molecule inhibitor has aroused great interests [29]. This study elucidated that histone methyltransferases EZH2/EHMT2 exerted synergistic promoting effects on the transformation of MDS to AML.

EZH2 as a histone methyltransferase, exerts effects on the equilibrium between self-renewal and differentiation of hematopoietic stem cells [30] and represents an independent prognostic factor of MDS [31]. EHMT2 can interact with transcription factors and participate in the regulation of MDS and AML [32]. We showed that EZH2 expression was reduced in bone marrow of MDS patients and promoted in MDS-AML patients, and EHMT2 was always highly expressed in MDS and MDS-AML patients. Additionally, NHD13 mice showed decreased EZH2 expression and increased EHMT2 expression. NHD13 mice with high expression of EZH2 or EHMT2 rapidly transformed from MDS to AML in a short time, and the survival rate was notably reduced. He et al. have also clarified that EZH2 is associated with drug resistance and deterioration of MDS, as well as the progression from MDS to AML [33]. Bernhard Lehnertz et al. have shown that EHMT2 inhibitor can significantly delay the progression of disease and reduce the frequency of leukemia stem cells in a mouse model of AML [34]. These results suggested that the expressions of EZH2/EHMT2 were concerned with the transformation from MDS to AML, and EZH2 and EHMT2 might have a synergistic relationship.

There is an interplay between EZH2 and EHMT2 to jointly maintain the silence of developmental gene subset [16]. The recent publication provides a strong theoretical basis to demonstrate that the dual inhibition of EZH2/EHMT2 methyltransferases can bring more effective prospects for cancer treatment [12]. Consistently, we showed that silencing of EZH2/EHMT2 expression significantly reduced SKM-1 cell

proliferation and blocked cell cycle. Hoxa9 is a homeodomain transcription factor, which plays a critical role in normal hematopoiesis and AML, and its overexpression is closely related to poor prognosis [35]. We found that Hoxa9 expression was positively correlated with the proliferation ability of SKM-1 cells. Deletion of EZH2/EHMT2 inhibited Hoxa9 expression. EZH2 knockout hinders the transformation of AML via repressing Hoxa9 expression [11]. Loss of EHMT2 attenuates Hoxa9-dependent transcription to inhibit proliferation and self-renewal of AML cells [34].

EZH2 establishes H3K27me3 markers on specific genes to promote the transcriptional inhibition of target genes [30]. H3K27me3 level was increased notably when EZH2 was overexpressed, but it also maintained a certain level when EZH2 was interfered. Repression of EZH2 reduces H3K27me3 level and induces curcumin resistance, but weakens leukemia transformation *in vivo* [36]. The effect of EZH2 deficiency may be limited due to EZH1 compensation and overlapping mechanism of transformation [24]. The biological significance of EZH1 is viewed as a backup enzyme of EZH2, which can make up for EZH2 deficiency in transcriptional inhibition in hematopoietic cells [37–39]. EZH1 expression in SKM-1 cells was increased significantly in the absence of EZH2. Downregulation of EZH2 reduced the level of H3K27me3 in SKM-1 cells after intervention of EZH1 expression. EZH1 targets bivalent genes to sustain the self-renewal of stem cells in EZH2-deficient MDS [40]. Briefly, EZH2 regulated the level of H3K27me3, and EZH1 compensated for the effect of EZH2 deletion. Similar to EZH2, EHMT2 inhibits the transcription of tumor suppressors by promoting the levels of H3K9me1/H3K9me2 [25]. H3K9me1/H3K9me2 level in SKM-1 cells were reduced significantly after intervention of EHMT2. EZH2/EHMT2 exert effects on SKM-1 cell proliferation by modulating the H3K27me3 and H3K9me1/H3K9me2 level.

Edward Curry et al. have revealed that EZH2/EHMT2 dual inhibition induces gene transcription and inhibits cancer cell growth [17]. The DLX genes serve as DNA-binding transcriptional regulators, controlling considerable downstream effector genes [41]. Notably, DLX5 hypermethylation is reported to be a common event in AML and MDS, and also concerned with the transformation from MDS to leukemia [26]. We showed that dual inhibition of EZH2 and EHMT2 in SKM-1 cells elevated the DLX5 expression to the highest level. DLX5 expression is upregulated by methyltransferase inhibitors during odontogenic differentiation of human dental pulp cells [42]. And upregulation of DLX5 could repress SKM-1 cell proliferation. Zhang et al. have also exhibited that DLX5 has antiproliferative and pro-apoptotic influences on SKM-1 cells [26]. Moreover, we found that DLX5 expression was negatively correlated with the Hoxa9 expression. Briefly, EZH2/EHMT2 synergistically catalyzed H3K27me3/H3K9me2 to inhibit the transcription of DLX5 and promoted the transformation from MDS to AML.

To sum up, EZH2/EHMT2 catalyzed H3K27me3/H3K9me2 to inhibit the transcription of DLX5, thus promoting the transformation from MDS to AML. This pilot study may provide theoretical holds for the EZH2/EHMT2-based regimens of MDS patients. In the future, we shall carry out more prospective trials on the feasibility and safety of EZH2/EHMT2 inhibitor in the treatment of MDS, so as to refine our clinical guidance.

Declarations

Acknowledgements

Not applicable.

Funding

This study was supported by Shanxi Province Applied Basic Research: Natural Science Foundation; The relationship between molecular biology abnormalities based on epigenetic modifiers and mRNA precursor splicing factors and the prognosis of myelodysplastic syndromes (No. 201801D121330). The funding body didn't participate in the design of the study and collection, analysis, and interpretation of data and in writing the manuscript.

Declaration of Competing Interest

The authors declare that they have no conflicts of interest.

Authors' Contributions

ZZZ is the guarantor of integrity of the entire study; YPM contributed to the study concepts, WLC study design, ZZZ definition of intellectual content and contributed to the literature research, LL contributed to the manuscript preparation and ZZZ contributed to the manuscript editing and YPM review; LL contributed to the clinical studies; GXL, YFZ and FGR contributed to the experimental studies; CXD data acquisition; WLC contributed to the data analysis and statistical analysis. All authors read and approved the final manuscript.

Data Availability Statement

All the data generated or analyzed during this study are included in this published article.

References

1. Ogawa S. Genetics of MDS. Blood. 2019;133:1049-1059.
2. Griffiths EA,Gore SD. Epigenetic therapies in MDS and AML. Adv Exp Med Biol. 2013;754:253-283.
3. Platzbecker U, Avvisati G, Cicconi L*, et al*. Improved Outcomes With Retinoic Acid and Arsenic Trioxide Compared With Retinoic Acid and Chemotherapy in Non-High-Risk Acute Promyelocytic Leukemia: Final Results of the Randomized Italian-German APL0406 Trial. J Clin Oncol. 2017;35:605-612.
4. Kubasch AS,Platzbecker U. Beyond the Edge of Hypomethylating Agents: Novel Combination Strategies for Older Adults with Advanced MDS and AML. Cancers (Basel). 2018;10:
5. Cao H, Li L, Yang D*, et al*. Recent progress in histone methyltransferase (G9a) inhibitors as anticancer agents. Eur J Med Chem. 2019;179:537-546.
6. Albert M,Helin K. Histone methyltransferases in cancer. Semin Cell Dev Biol. 2010;21:209-220.

7. Wei Y, Ganan-Gomez I, Salazar-Dimicoli S, *et al*. Histone methylation in myelodysplastic syndromes. Epigenomics. 2011;3:193-205.
8. Abou Zahr A, Saad Aldin E, Barbarotta L, *et al*. The clinical use of DNA methyltransferase inhibitors in myelodysplastic syndromes. Expert Rev Anticancer Ther. 2015;15:1019-1036.
9. Tremblay-LeMay R, Rastgoo N, Pourabdollah M, *et al*. EZH2 as a therapeutic target for multiple myeloma and other haematological malignancies. Biomark Res. 2018;6:34.
10. de Souza Fernandez T, Fonseca Alvarenga T, Almeida Antonio de Kos E, *et al*. Aberrant Expression of EZH2 in Pediatric Patients with Myelodysplastic Syndrome: A Potential Biomarker of Leukemic Evolution. Biomed Res Int. 2019;2019:3176565.
11. Sashida G, Harada H, Matsui H, *et al*. Ezh2 loss promotes development of myelodysplastic syndrome but attenuates its predisposition to leukaemic transformation. Nat Commun. 2014;5:4177.
12. Soumyanarayanan U,Dymock BW. Recently discovered EZH2 and EHMT2 (G9a) inhibitors. Future Med Chem. 2016;8:1635-1654.
13. Cho HS, Kelly JD, Hayami S, *et al*. Enhanced expression of EHMT2 is involved in the proliferation of cancer cells through negative regulation of SIAH1. Neoplasia. 2011;13:676-684.
14. Ding J, Li T, Wang X, *et al*. The histone H3 methyltransferase G9A epigenetically activates the serine-glycine synthesis pathway to sustain cancer cell survival and proliferation. Cell Metab. 2013;18:896-907.
15. Pappano WN, Guo J, He Y, *et al*. The Histone Methyltransferase Inhibitor A-366 Uncovers a Role for G9a/GLP in the Epigenetics of Leukemia. PLoS One. 2015;10:e0131716.
16. Mozzetta C, Pontis J, Fritsch L, *et al*. The histone H3 lysine 9 methyltransferases G9a and GLP regulate polycomb repressive complex 2-mediated gene silencing. Mol Cell. 2014;53:277-289.
17. Curry E, Green I, Chapman-Rothe N, *et al*. Dual EZH2 and EHMT2 histone methyltransferase inhibition increases biological efficacy in breast cancer cells. Clin Epigenetics. 2015;7:84.
18. Kopaladze RA. [Methods for the euthanasia of experimental animals--the ethics, esthetics and personnel safety]. Usp Fiziol Nauk. 2000;31:79-90.
19. Zatroch KK, Knight CG, Reimer JN, *et al*. Refinement of intraperitoneal injection of sodium pentobarbital for euthanasia in laboratory rats (Rattus norvegicus). BMC Vet Res. 2017;13:60.
20. Dagdemir A, Durif J, Ngollo M, *et al*. Histone lysine trimethylation or acetylation can be modulated by phytoestrogen, estrogen or anti-HDAC in breast cancer cell lines. Epigenomics. 2013;5:51-63.
21. Lin YW, Slape C, Zhang Z, *et al*. NUP98-HOXD13 transgenic mice develop a highly penetrant, severe myelodysplastic syndrome that progresses to acute leukemia. Blood. 2005;106:287-295.
22. Slape C, Liu LY, Beachy S, *et al*. Leukemic transformation in mice expressing a NUP98-HOXD13 transgene is accompanied by spontaneous mutations in Nras, Kras, and Cbl. Blood. 2008;112:2017-2019.
23. Hosono N. Genetic abnormalities and pathophysiology of MDS. Int J Clin Oncol. 2019;24:885-892.

24. Ling VY, Saw J, Tremblay CS, *et al*. Attenuated Acceleration to Leukemia after Ezh2 Loss in Nup98-HoxD13 (NHD13) Myelodysplastic Syndrome. Hemasphere. 2019;3:e277.
25. Kondengaden SM, Luo LF, Huang K, *et al*. Discovery of novel small molecule inhibitors of lysine methyltransferase G9a and their mechanism in leukemia cell lines. Eur J Med Chem. 2016;122:382-393.
26. Zhang TJ, Xu ZJ, Gu Y, *et al*. Identification and validation of prognosis-related DLX5 methylation as an epigenetic driver in myeloid neoplasms. Clin Transl Med. 2020;
27. Haroun F, Solola SA, Nassereddine S, *et al*. PD-1 signaling and inhibition in AML and MDS. Ann Hematol. 2017;96:1441-1448.
28. Maegawa S, Gough SM, Watanabe-Okochi N, *et al*. Age-related epigenetic drift in the pathogenesis of MDS and AML. Genome Res. 2014;24:580-591.
29. Xu F,Li X. The role of histone methyltransferase EZH2 in myelodysplastic syndromes. Expert Rev Hematol. 2012;5:177-185.
30. Safaei S, Baradaran B, Hagh MF, *et al*. Double sword role of EZH2 in leukemia. Biomed Pharmacother. 2018;98:626-635.
31. Nazha A, Narkhede M, Radivoyevitch T, *et al*. Incorporation of molecular data into the Revised International Prognostic Scoring System in treated patients with myelodysplastic syndromes. Leukemia. 2016;30:2214-2220.
32. Spensberger D,Delwel R. A novel interaction between the proto-oncogene Evi1 and histone methyltransferases, SUV39H1 and G9a. FEBS Lett. 2008;582:2761-2767.
33. Liu J, Jiang T, He M, *et al*. Andrographolide prevents human nucleus pulposus cells against degeneration by inhibiting the NF-kappaB pathway. J Cell Physiol. 2019;234:9631-9639.
34. Lehnertz B, Pabst C, Su L, *et al*. The methyltransferase G9a regulates HoxA9-dependent transcription in AML. Genes Dev. 2014;28:317-327.
35. Collins CT,Hess JL. Deregulation of the HOXA9/MEIS1 axis in acute leukemia. Curr Opin Hematol. 2016;23:354-361.
36. Ma L, Zhang X, Wang Z, *et al*. Anti-cancer Effects of Curcumin on Myelodysplastic Syndrome through the Inhibition of Enhancer of Zeste Homolog-2 (EZH2). Curr Cancer Drug Targets. 2019;19:729-741.
37. Ezhkova E, Lien WH, Stokes N, *et al*. EZH1 and EZH2 cogovern histone H3K27 trimethylation and are essential for hair follicle homeostasis and wound repair. Genes Dev. 2011;25:485-498.
38. Margueron R, Li G, Sarma K, *et al*. Ezh1 and Ezh2 maintain repressive chromatin through different mechanisms. Mol Cell. 2008;32:503-518.
39. Mochizuki-Kashio M, Aoyama K, Sashida G, *et al*. Ezh2 loss in hematopoietic stem cells predisposes mice to develop heterogeneous malignancies in an Ezh1-dependent manner. Blood. 2015;126:1172-1183.
40. Aoyama K, Oshima M, Koide S, *et al*. Ezh1 Targets Bivalent Genes to Maintain Self-Renewing Stem Cells in Ezh2-Insufficient Myelodysplastic Syndrome. iScience. 2018;9:161-174.

41. Kraus P,Lufkin T. Dlx homeobox gene control of mammalian limb and craniofacial development. Am J Med Genet A. 2006;140:1366-1374.
42. Zhang D, Li Q, Rao L, *et al*. Effect of 5-Aza-2'-deoxycytidine on odontogenic differentiation of human dental pulp cells. J Endod. 2015;41:640-645.

Figures

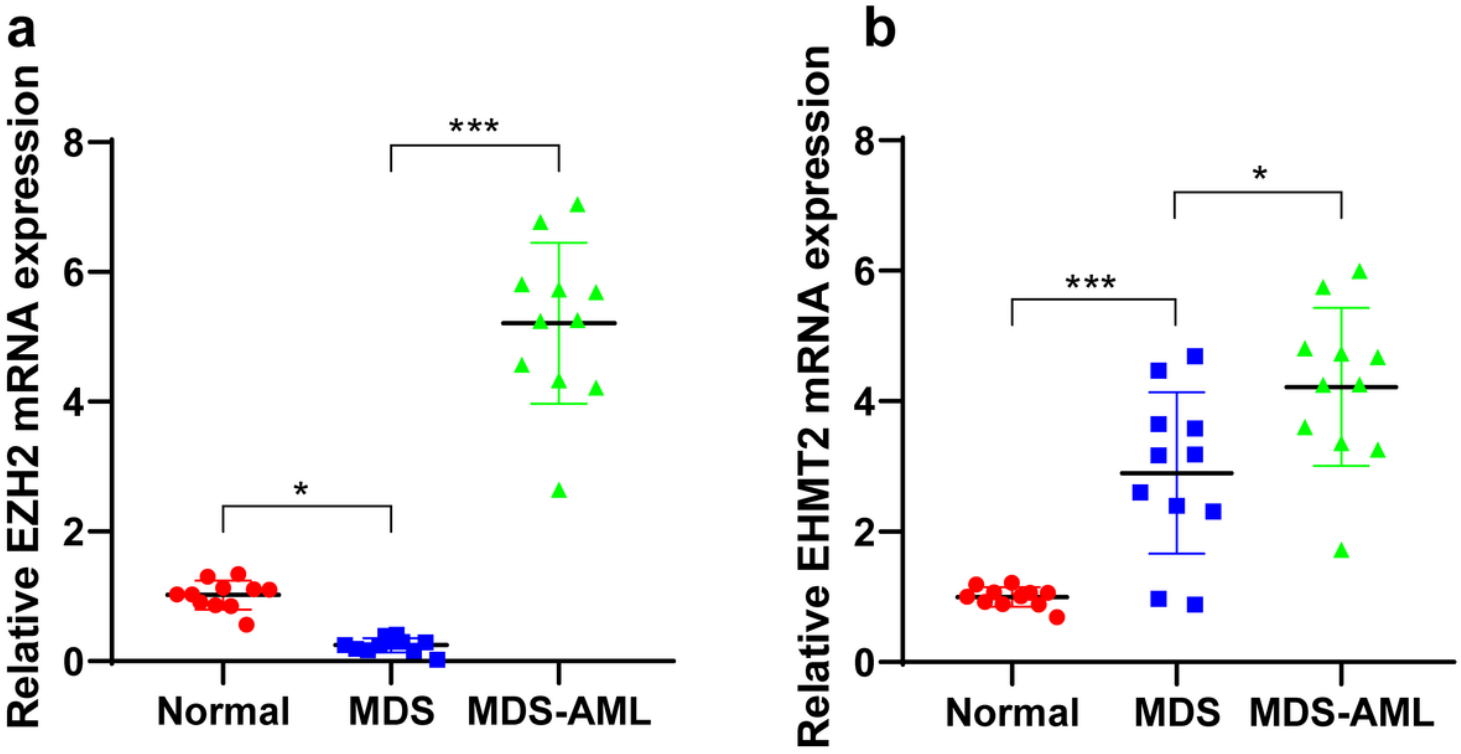

Figure 1

EZH2 was downregulated in MDS patients and upregulated in MDS-AML patients. A-B: expressions of EZH2 and EHMT2 in bone marrow of MDS patients, MDS-AML patients and non-cancer individuals were detected using RT-qPCR. Data are analyzed using one-way ANOVA, followed by Tukey's multiple comparisons test, *p < 0.05, ***p < 0.001.

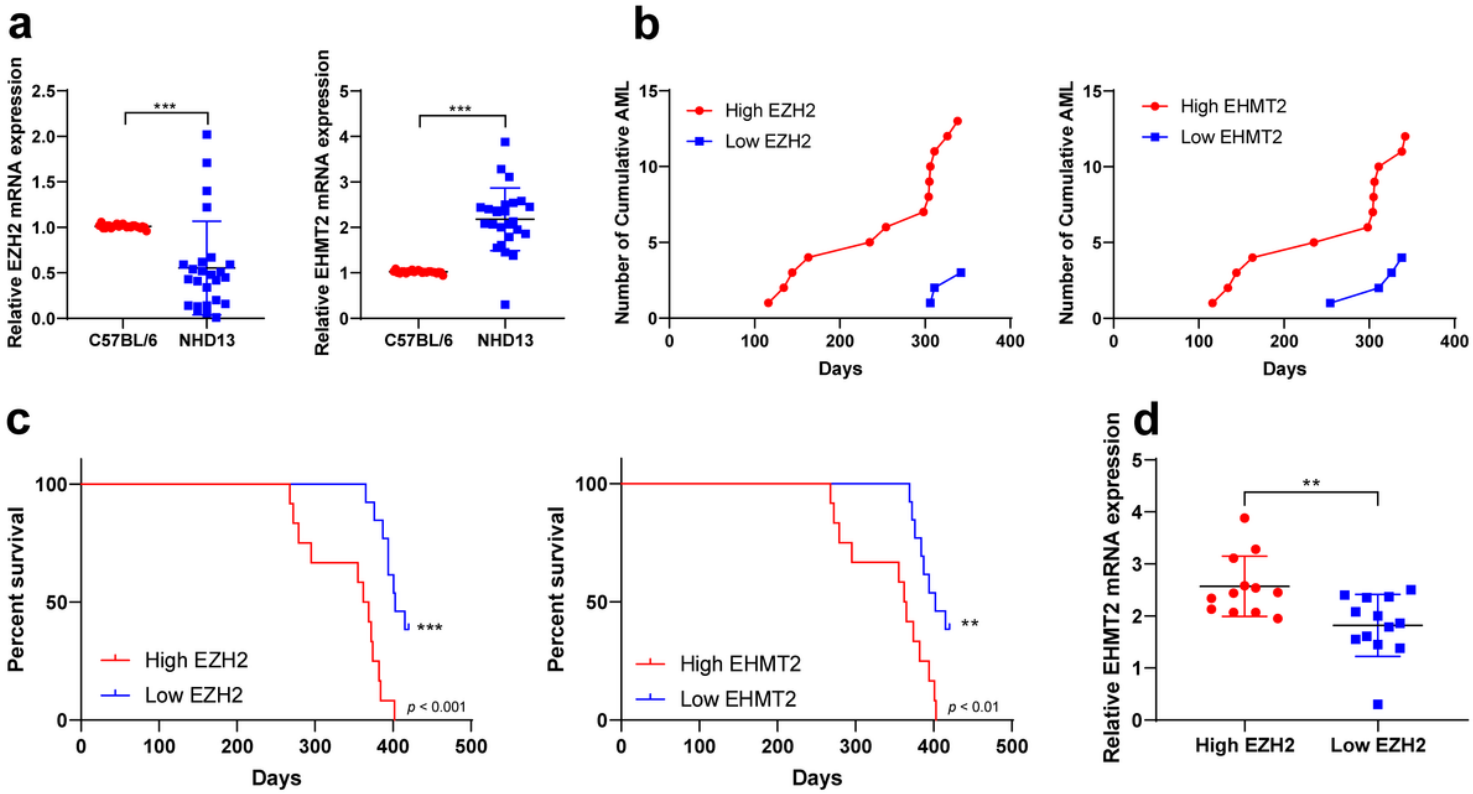

Figure 2

NHD13 mice with high expression of EZH2 transformed into AML more quickly. A: the expressions of EZH2 and EHMT2 in peripheral blood of mice (at the age of 4 months) were detected using RT-qPCR; B: according to the median expressions of EZH2 and EHMT2, mice were divided into high/low groups, and the time of transforming from MDS into AML of mice in different groups within 14 months was recorded; C: survival curves were used to analyze the survival rates of mice in different groups; D: expression of EHMT2 in peripheral blood of mice in high/low EZH2 groups was compared. N = 25. Data in panels A/D are analyzed using t test, **p < 0.01, ***p < 0.001.

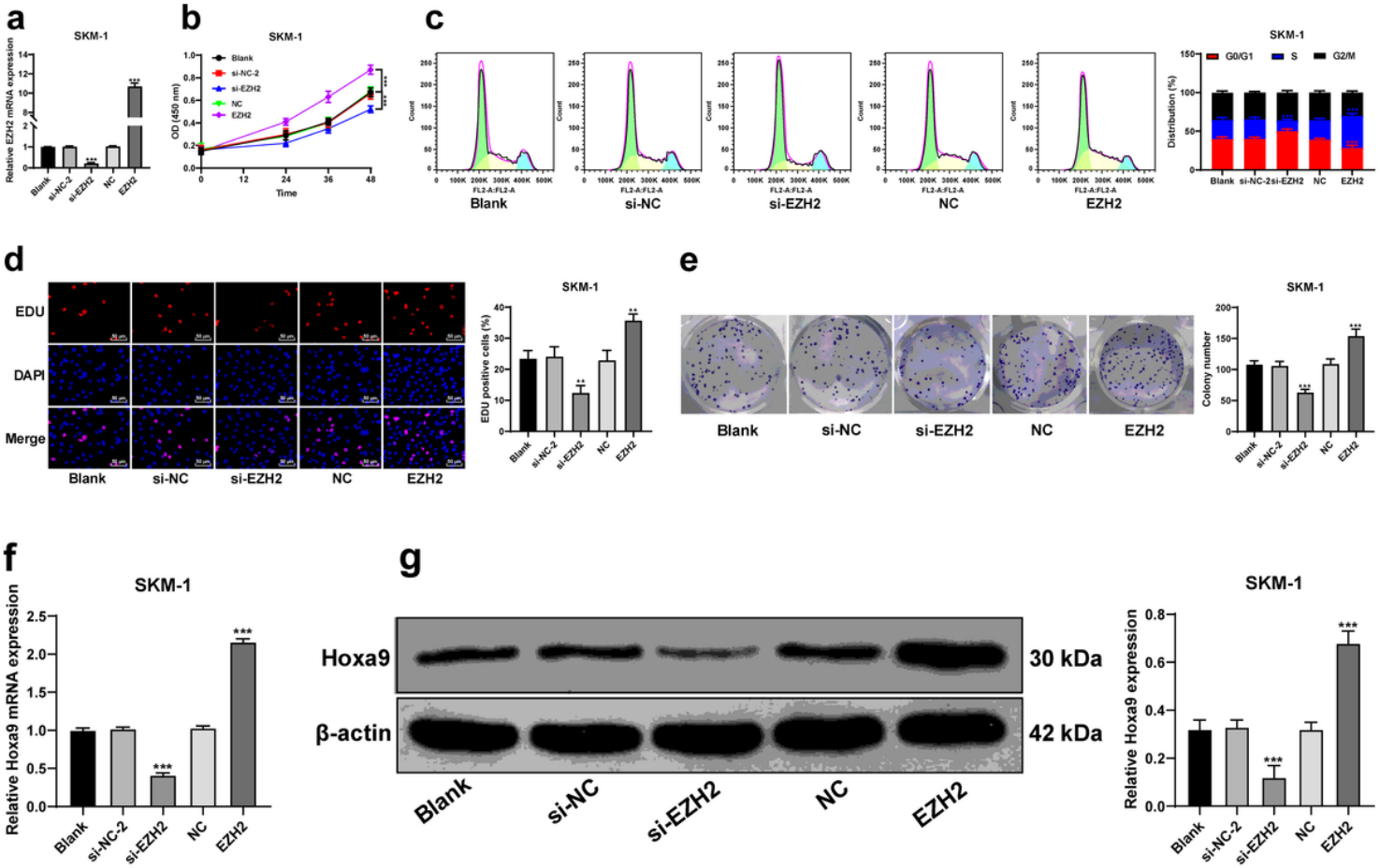

Figure 3

Silencing EZH2 expression inhibited SKM-1 cell proliferation. A: transfection efficiency of si-EZH2 or overexpression of EZH2 was confirmed using RT-qPCR; B: viability of SKM-1 cells under different treatments was measured using CCK-8 assay; C: cell cycle of SKM-1 cells was detected using flow cytometry; D/E: proliferation ability of SKM-1 cells was measured using EdU and colony formation assay; F/G: Hoxa9 expression in SKM-1 cells was detected using RT-qPCR and Western blot analysis. The cell experiments were repeated three times. Data are expressed as mean ± standard deviation. Data in panels A/D/E/F/G were analyzed using one-way ANOVA, and data in panels B/C were analyzed using two-way ANOVA, followed by Tukey's multiple comparisons test, *p < 0.05, **p < 0.01, ***p < 0.001 vs. blank group.

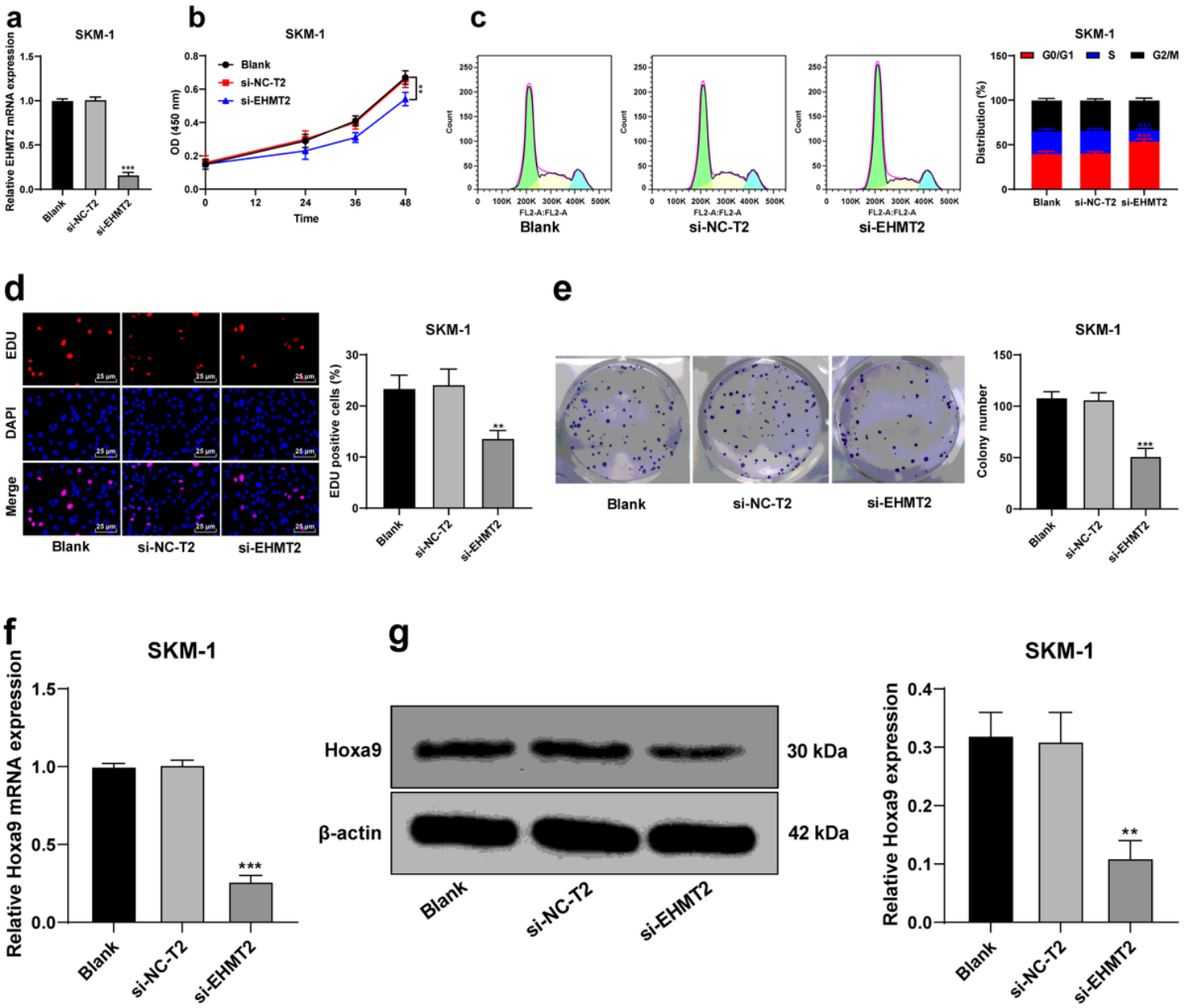

Figure 4

Silencing EHMT2 expression inhibited SKM-1 cell proliferation. A: transfection efficiency of si-EHMT2 or overexpression of EHMT2 was confirmed using RT-qPCR; B: viability of SKM-1 cells under different treatments was measured using CCK-8 assay; C: cell cycle of SKM-1 cells was detected using flow cytometry; D/E: proliferation ability of SKM-1 cells was measured using EdU and colony formation assay; F/G: Hoxa9 expression in SKM-1 cells was detected using RT-qPCR and Western blot analysis. The cell experiments were repeated three times. Data are expressed as mean ± standard deviation. Data in panels A/D/E/F/G were analyzed using one-way ANOVA, and data in panels B/C were analyzed using two-way ANOVA, followed by Tukey's multiple comparisons test, *p < 0.05, **p < 0.01, ***p < 0.001 vs. blank group.

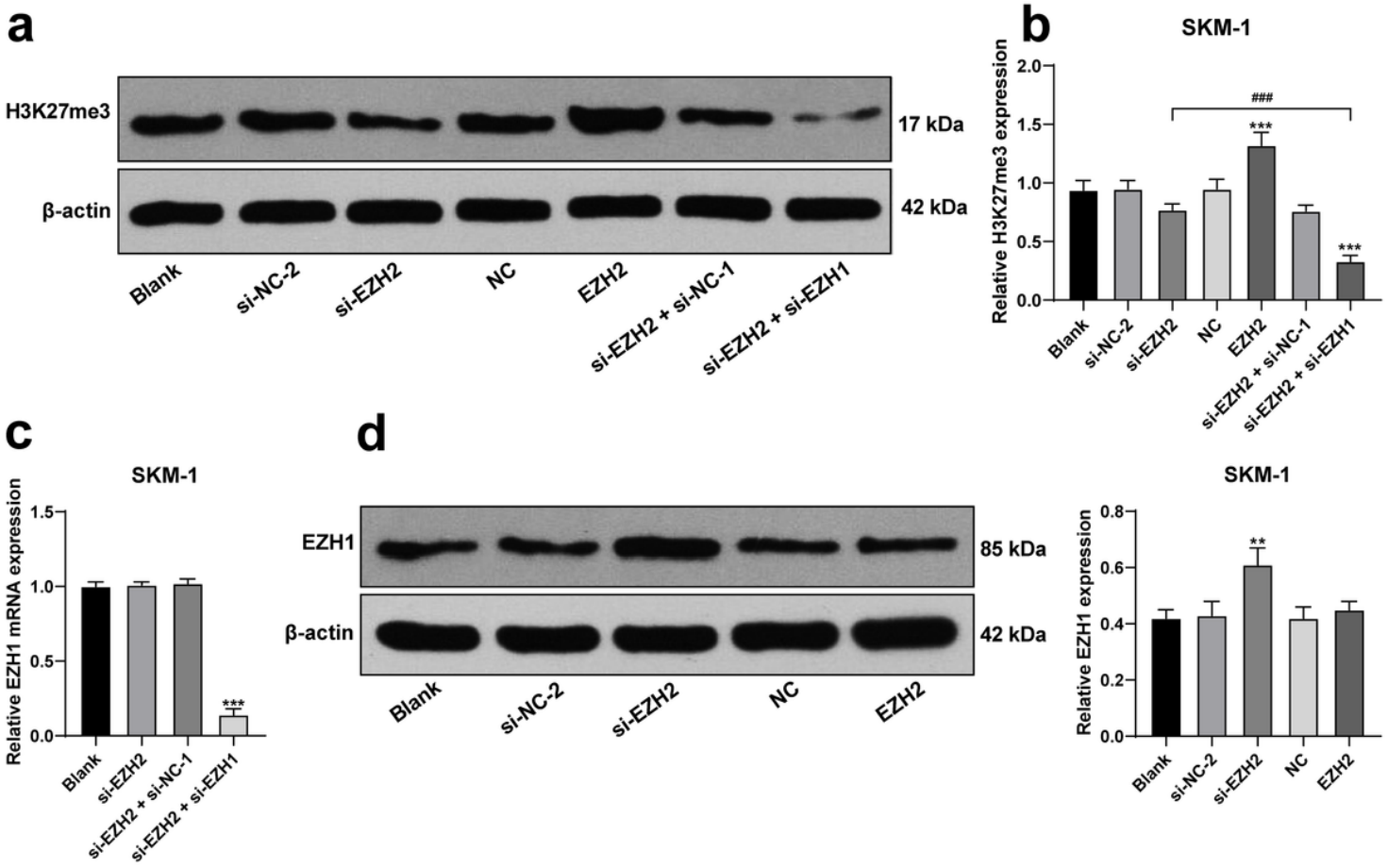

Figure 5

EZH2 regulated H3K27me3 level and EZH1 compensated for the effect of EZH2 deficiency. A/B/D: protein levels of EZH2, H3K27me3 and EZH1 in SKM-1 cells were measured using Western blot analysis; C: expression of EZH1 in SKM-1 cells was detected using RT-qPCR. The cell experiments were repeated three times. Data were analyzed using one-way ANOVA, followed by Tukey's multiple comparisons test, **p < 0.01, ***p < 0.001 vs. blank group; ###p < 0.001 vs. for group pair comparison.

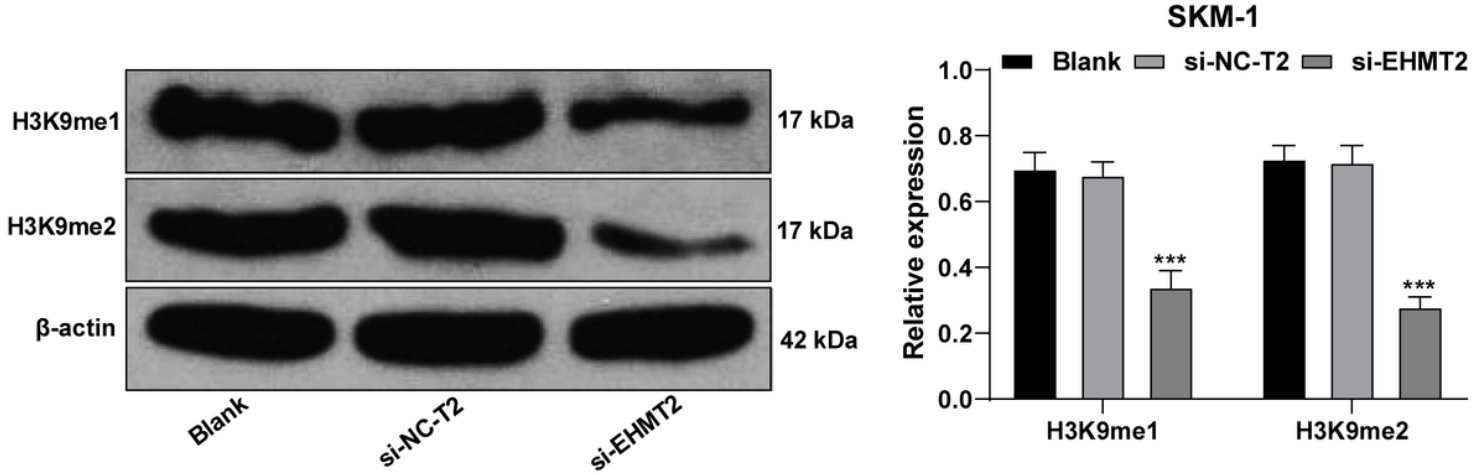

Figure 6

EHMT2 positively regulated H3K9me1/H3K9me2 level. Protein levels of H3K9me1/H3K9me2 in SKM-1 cells were measured using Western blot analysis. The cell experiments were repeated three times. Data were analyzed using two-way ANOVA, followed by Tukey's multiple comparisons test, ***p < 0.001 vs. blank group.

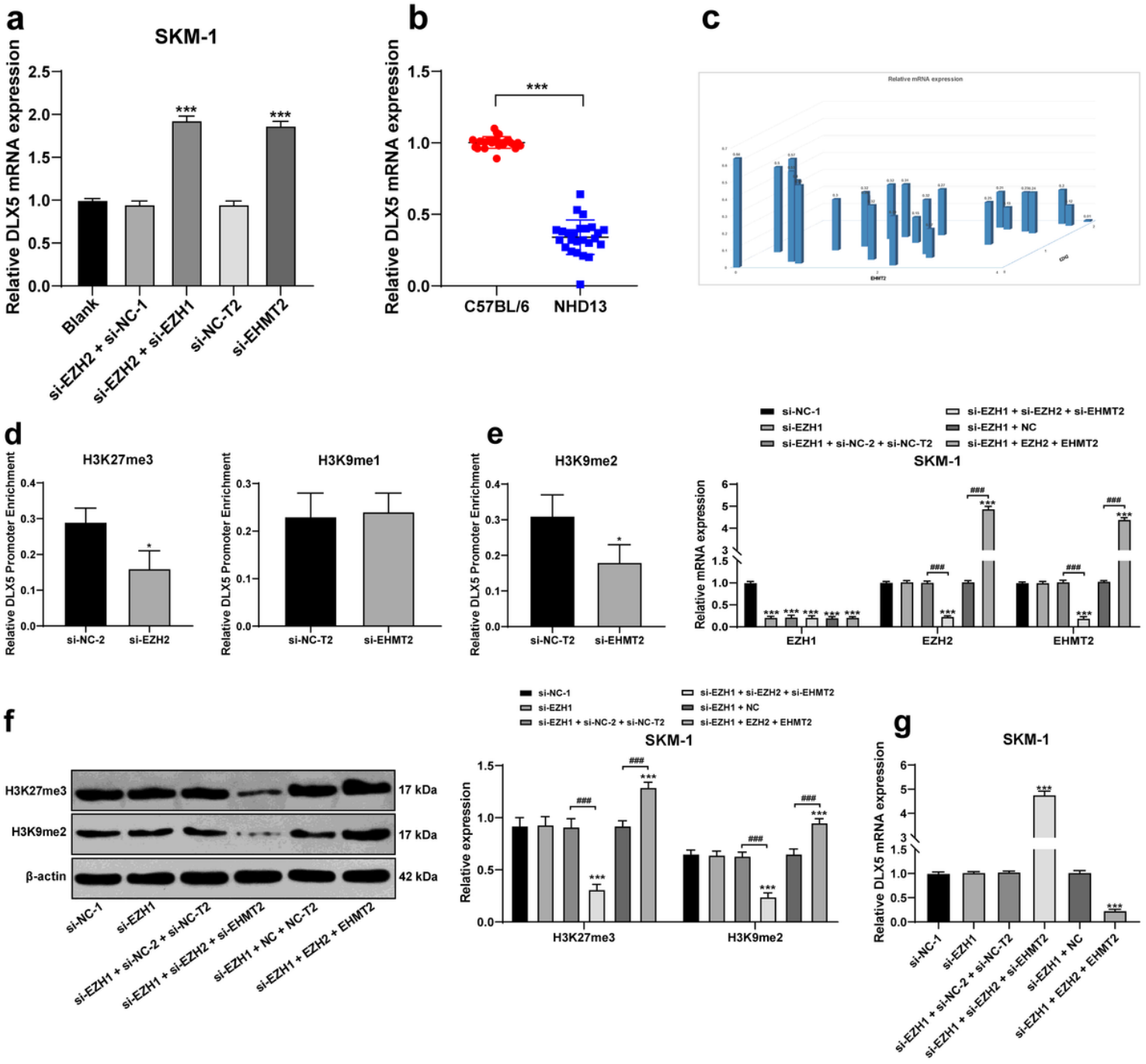

Figure 7

EZH2 and EHMT2 synergistically inhibited DLX5 gene transcription. A: DLX5 mRNA level in SKM-1 cells was detected using RT-qPCR; B: DLX5 mRNA level in NHD13 mice and C57BL/6 mice was detected using

RT-qPCR; C: DLX5 mRNA level was increased to the highest level when EZH2 and EHMT2 were at low expressions at the same time, and decreased to the lowest level when EZH2 and EHMT2 were at high expressions, with the X-axis representing EHMT2, the Y-axis representing EZH2, and the Z-axis representing DLX5; D: binding levels of DLX5 promoter region with H3K27me3, H3K9me1 and H3K9me2 were detected using ChIP; the histogram showed that the binding content of DLX5 promoter in DNA IP was detected using RT-qPCR after ChIP experiment, which was represented by the relative content of DNA input; E: expressions of EZH1, EZH2 and EHMT2 in SKM-1 cells were detected using RT-qPCR; F: expressions of H3K27me3 and H3K9me2 in SKM-1 cells were detected using Western blot analysis; G: DLX5 mRNA level in SKM-1 cells was detected using RT-qPCR. The cell experiments were repeated three times. Data in panels A/B/D/G were analyzed using one-way ANOVA, and data in panels E/F were analyzed using two-way ANOVA, followed by Tukey's multiple comparisons test, ***p < 0.001 vs. si-NC-1 group; ###p < 0.001 vs. for group pair comparison.

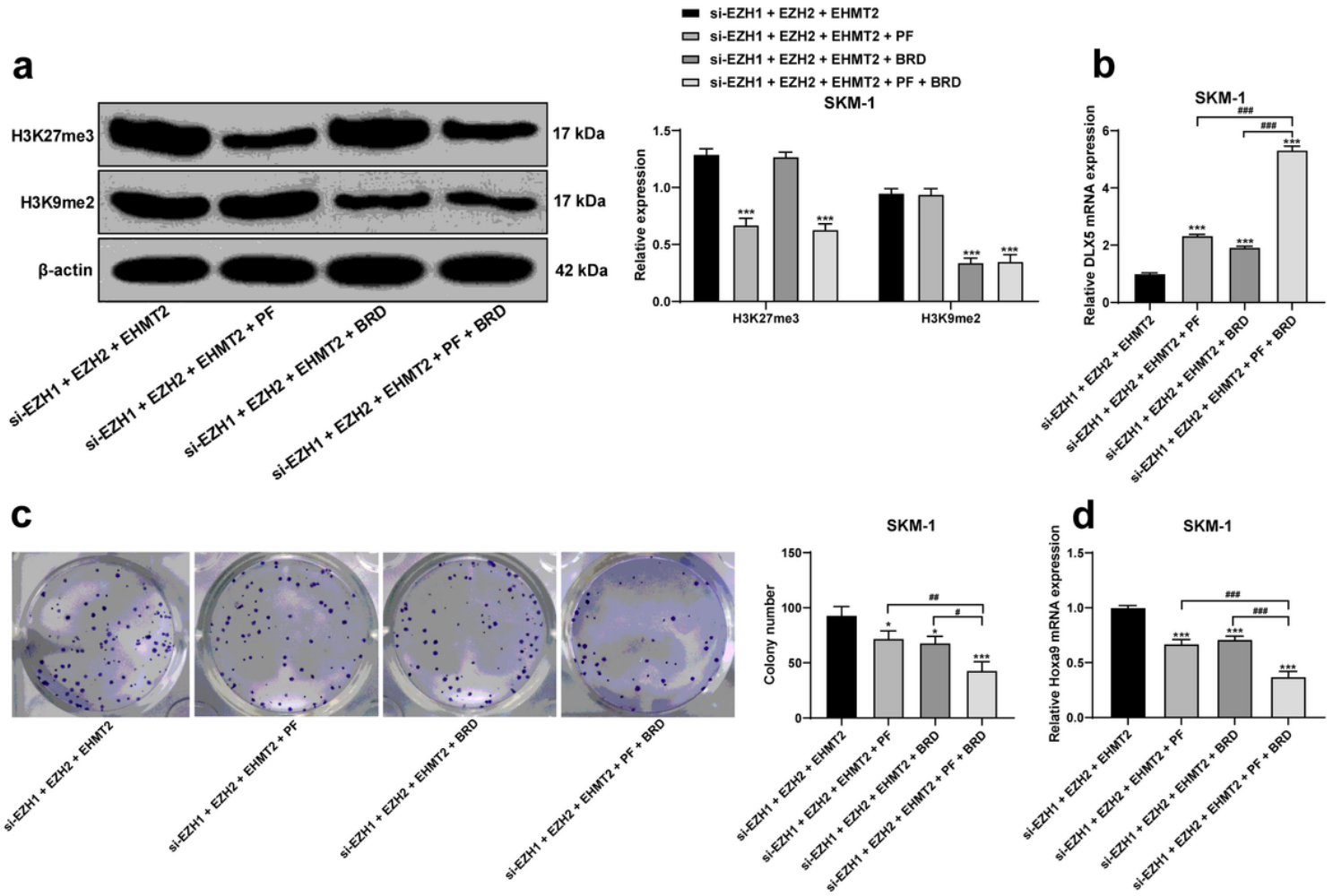

Figure 8

Histone demethylation enhanced DLX5 expression and inhibited SKM-1 cell proliferation. A: histone methylation and levels of H3K27me3 and H3K9me2 were measured using Western blot analysis; PF (PF-06726304) was H3K27me3 inhibitor and BRD (BRD4770) was H3K9me2 inhibitor; B/D: expressions of DLX5 and Hoxa9 were detected using RT-qPCR; C: proliferation ability of SKM-1 cells was measured using

colony formation assay. The cell experiments were repeated three times. Data in panels B/C/D were analyzed using one-way ANOVA, and data in panel A were analyzed using two-way ANOVA, followed by Tukey's multiple comparisons test, *p < 0.05, **p < 0.01, ***p < 0.001 vs. blank group; ###p < 0.001 vs. adjacent groups.

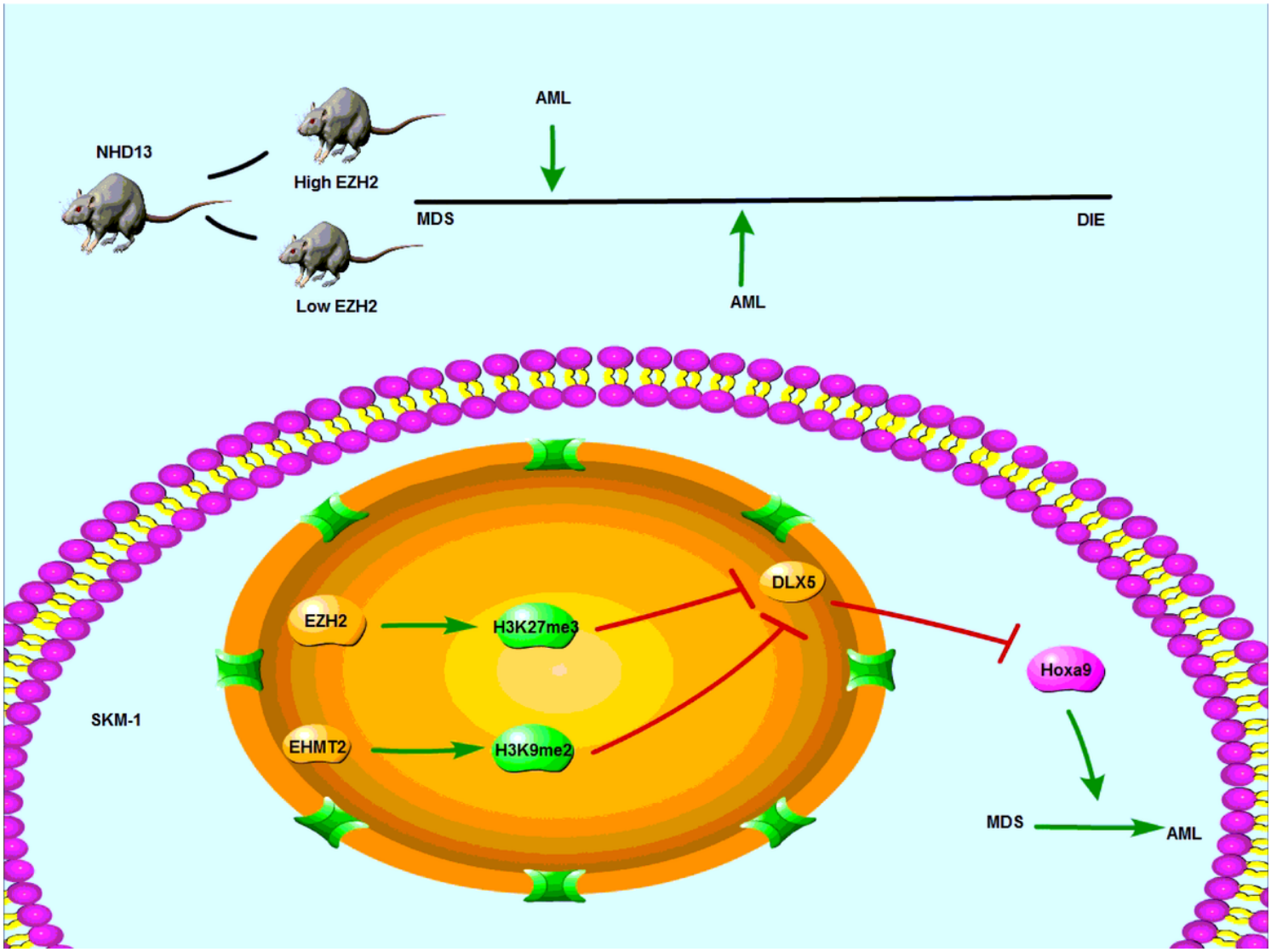

Figure 9

Mechanism diagram. EZH2 and EHMT2 synergistically regulated DLX5 transcription and promoted the transition from MDS to AML.